

Preparation and catalytic properties of ZrO_2 - Al_2O_3 composite oxide supported nickel catalysts for methane reforming with carbon dioxide

HAO Zheng-ping^{1,*}, HU Chun¹, JIANG Zheng¹, G. Q. LU²

(1. Research Center for Eco-Environmental Sciences, Chinese Academy of Sciences, Beijing 100085, China. E-mail: zpinghao@mail.rcees.ac.cn;

2. Department of Chemical Engineering, University of Queensland, St. Lucia, QLD 4072, Australia)

Abstract: ZrO_2 - Al_2O_3 composite oxides and supported Ni catalysts were prepared, and characterized by N_2 adsorption/desorption, X-ray diffraction (XRD) and X-ray photoelectron spectroscopy (XPS) techniques. The catalytic performance and carbon deposition was also investigated. This mesoporous composite oxide is shown to be a promising catalyst support. An increase in the catalytic activity and stability of methane and carbon dioxide reforming reaction was resulted from the zirconia addition, especially at 5wt% ZrO_2 content. The Ni catalyst supported ZrO_2 - Al_2O_3 has a strong resistance to sintering and the carbon deposition in a relatively long-term reaction.

Keywords: oxides; catalytic properties; methane reforming; carbon deposition

Introduction

The reforming reaction of methane with carbon dioxide into synthesis gas is a very attractive route for the production of chemicals and energy storage. It is suitable for the production of CO-rich synthesis gas, which can be used in Fisher-Tropsch synthesis, for methanol, and dimethylether production. This reaction has important environmental implications as two greenhouse gases are converted into a valuable feedstock. It is becoming important because it offers several advantages over the process of steam reforming or partial oxidation of methane. This process also exhibits a certain potential to be used as thermochemical heat-pipe for recovery, storage and transmission of solar and other renewable energy sources.

It is well known that supported group VIII metals are good catalysts for the reforming reaction. One serious problem, though, is the catalyst deactivation due to carbon deposition, especially for Ni-based catalysts (Wang, 1998). However, from the viewpoint of industrial application, nickel-supported catalysts are found to be promising and relatively cheaper catalysts for methane reforming with carbon dioxide. Therefore, development of stable anti-carbon Ni catalysts is of great interest.

Several studies have shown that the nature of catalyst support employed influences the catalytic behaviors and carbon deposition. Introduction of rare earth or alkaline oxides to Ni catalysts have already shown improvement in their coking-resistance (Cheng, 1996; Chudhary, 1995; Ruckenstein, 1996; Zhang, 1995). Seshan *et al.* (Seshan, 1994) studied a series of Ni/ ZrO_2 catalysts for the CO_2 reforming of methane and found that catalysts with high loading nickel deactivated quickly because of coking. Lercher (Lercher, 1996) reported that ZrO_2 was crucial for platinum and nickel catalysts to minimize coke deposition under CO_2/CH_4 reforming condition, and a well-dispersed ZrO_2 -supported nickel catalyst seemed to be a viable alternative to noble metal catalysts. Wei and Xu (Wei, 2000) researched Ni/ ZrO_2 catalysts with different preparations for CO_2 reforming of methane and found that catalytic stability depends greatly on the preparation method and the support precursor. They reported that the catalyst prepared by impregnation of ultra-fine $Zr(OH)_4$ particles with nickel nitrate showed high and extremely stable activity for syngas production. Li *et al.* (Li, 1999a; 1999b) studied the performance of CO_2 reforming of methane and carbon deposition on Ni/ ZrO_2 catalyst support by

means of dilution methods for catalyst and reactants.

However, ZrO_2 is not suitable as a catalyst support on a commercial scale because of its cost (Wang, 1999). In recent years, the study of special properties of metal catalysts supported on composite oxides has aroused great attention. These works mainly concentrate on the interaction between the coated oxide and substrate. As the main composition of catalyst, the support usually affects the performance of catalyst significantly (Zhang, 1992; Hao, 2003). The introduction of the second oxide phase can modify the surface acidic and basic sites, adsorptive capacity, and thermal stability of substrate (Guo, 2000). As shown in a recent thorough review (Bradford, 1999), the reforming of CH_4 and CO_2 has been extensively studied using composite oxide catalyst support, such as $CaO-Al_2O_3$, $MgO-CaO-Al_2O_3$, $Ce_2O_3-Al_2O_3$, $La_2O_3-Al_2O_3$, $MgO-Al_2O_3$, $SiO_2-Al_2O_3$, and $MgO-SiO_2$.

The aim of this work is to study the textural and structural characteristics of mesoporous ZrO_2 - Al_2O_3 composite oxide support and their supported Ni catalysts, as well as the effect of the composite support on the catalytic performance for the carbon dioxide reforming of methane to synthesis gas.

1 Experiment

1.1 Catalyst preparation

Composite supports were prepared by multi-impregnation of Al_2O_3 with $Zr(NO_3)_4$ solution. The samples were dried at 110 °C overnight, then calcined in air at 500 °C for 4 h. ZrO_2 content was in range of 1%–15wt%.

Supported Ni catalysts were prepared by the incipient wetness impregnation method with aqueous solutions of nitrates as metal precursors. The solids were dried in air at 105 °C overnight, and then calcined at 500 °C in air for 4 h in order to realize the complete decomposition of the nitrate. After this treatment, the catalyst was reduced at 500 °C in a stream of 50% H_2/N_2 for 2 h. The nickel metal loading of the catalyst was 9wt%.

1.2 Catalyst characterization

The surface area and pore size of the catalysts were determined by nitrogen adsorption using a NOVA 1200 (Quantachrome, USA) at -196 °C. The sample was degassed under vacuum of 10^{-2} torr at 230 °C for 4 h in high vacuum before the measurement. The surface area S was calculated using the BET equation. The total pore volume was derived from the amount of adsorption at a relative

pressure close to unity. The average pore size (D_p) was estimated from the pore volume assuming a cylindrical pore geometry using the equation, $R_p = 2V_{liq}/S$, where V_{liq} is the volume of liquid adsorbate contained in the pores and S is the BET surface area.

XRD powder diffraction measurements were performed on a PW 1050 Diffractometer Automation Site122D. The Scherrer equation was used to estimate the crystallite size.

X-ray photoelectron spectroscopic (XPS) analyses were carried out using a PHI Model 560 XPS/SAM/SIMS I multitechnique surface analysis system at the Brisbane Surface Analysis Facility (BSAF), University of Queensland. The system incorporates a PHI model 25—270AR CMA electron energy analyzer and a dual Mg/Al X-ray source. Atomic concentrations were calculated from the peak areas using linear baselines and in-house experimentally determined sensitivity factors.

Temperature programmed oxidation experiments of carbon species formed on the catalyst were conducted on a thermogravimetric analyzer (Shimadzu-TGA50) in air at 20 ml/min. The temperature was first raised to 110 °C, and kept there for 1 h, and then raised to 800 °C with a heating rate of 5 °C/min. In addition, the thermal stability of the composite oxide was also studied by the temperature programmed oxidation in air using TGA.

1.3 Catalytic performance

Catalytic reaction experiments were conducted in a vertical fixed-bed reactor made of quartz tube under atmospheric pressure. 0.2 g catalyst was placed in the quartz tube reactor. A thermocouple was placed in the tube with one end touching on the catalyst in order to measure the bed temperature. The mixture of reactants of methane and carbon dioxide with a ratio of 1/1 was fed into the reactor at the flow rate of 60 ml/min (GHSV = 18000 ml/(g·h)). The analyses of reactant/product mixtures were carried out using an on-line gas chromatograph (Shimadzu-17A) equipped with a thermal conductivity measure. A carbosphere (80—100 mesh) column was used to separate H₂, CO, CH₄, and CO₂. Prior to each reaction run the catalyst was reduced in situ at 500 °C in 50% H₂/N₂ for 2 h. The activities of catalysts were investigated at temperatures between 500—800 °C, and stability tests were conducted at a given reaction temperature.

2 Results and discussion

2.1 Variation of texture and structure for composite oxide supports and catalysts

Data of surface area and pore volume for ZrO₂-Al₂O₃ are listed in Table 1. The composite oxide with low ZrO₂ content showed higher surface area and larger pore volume, close to that of pure Al₂O₃. When the ZrO₂ content exceeded 2%, the surface area and pore volume decreased gradually. Similar to Guo's observation (Guo, 2000), the preparation process can reduce the surface area of Al₂O₃. The blocking of some pores of Al₂O₃ by crystallization can result in the decrease of surface area as well. Table 2 shows the data of surface area and pore volume for Ni/ZrO₂-Al₂O₃ catalysts. The order of surface area and pore volume for catalysts is similar to supports. It is also seen clearly that the surface area of the catalyst is generally reduced.

Table 1 Textural data of ZrO₂-Al₂O₃ support

ZrO ₂ content, wt%	Surface area, m ² /g	Pore volume, cm ³ /g	D, nm
0	112	0.286	10.3
1	105	0.245	10
2	100.5	0.24	9.7
5	98.4	0.234	9.5
8	95.2	0.218	9.2
10	94.3	0.221	9.4
15	90.6	0.223	9.9

Table 2 Textural variations of Ni/ZrO₂-Al₂O₃ catalysts

Catalyst	Surface area, m ² /g	Pore volume, cm ³ /g	D, nm
Ni/Al ₂ O ₃	118.5	0.23	7.8
Ni/2% ZrO ₂ -Al ₂ O ₃	86.4	0.24	10
Ni/5% ZrO ₂ -Al ₂ O ₃	85.1	0.234	9.5
Ni/8% ZrO ₂ -Al ₂ O ₃	81.6	0.208	10.4
Ni/10% ZrO ₂ -Al ₂ O ₃	80.6	0.183	9.1
Ni/15% ZrO ₂ -Al ₂ O ₃	78.1	0.19	10.1
Ni/2% ZrO ₂ -Al ₂ O ₃ (used)	18.4	0.078	19.8
Ni/5% ZrO ₂ -Al ₂ O ₃ (used)	59.5	0.163	11.2

The XRD patterns of ZrO₂-Al₂O₃ are shown in Fig. 1. The sample with 1% ZrO₂ showed no difference to the Al₂O₃ sample. A small quantity of ZrO₂ appeared in 2% ZrO₂-Al₂O₃. The peak characteristic of cubic ZrO₂ became larger with the increase in ZrO₂ content. This indicated that ZrO₂ was highly dispersed on the surface of Al₂O₃ at lower than 2%, and larger cubic ZrO₂ particles formed when the ZrO₂ content exceeded this value. This result is different from the report by Guo and Li (Guo, 2000). They found that the tetragonal ZrO₂ phase appeared when the ZrO₂ content is close to 10%. Perhaps the principal reason for this is the Al₂O₃ support we used with a relatively low surface area and the different preparation methods. The thermal stability of composite oxide was studied by TPO in a TGA, and the results are shown in Fig. 2. It can be seen that the thermal stability of 5% ZrO₂-Al₂O₃ is better than 2% ZrO₂-Al₂O₃ in air.

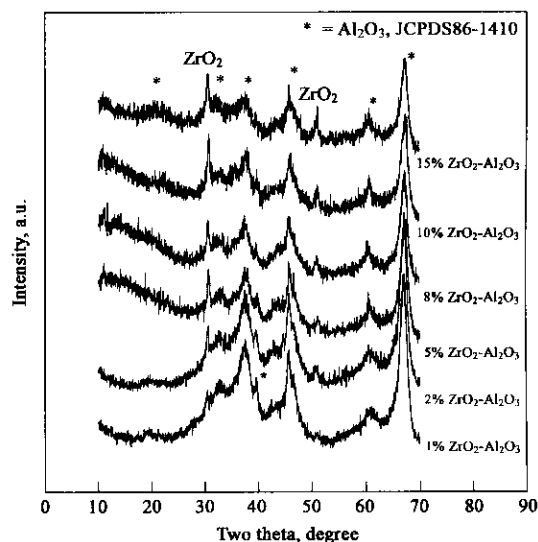


Fig. 1 XRD patterns of ZrO₂-Al₂O₃ supports

The XRD patterns of Ni/ZrO₂-Al₂O₃ catalysts are shown in Fig. 3. It can be observed that Ni/Al₂O₃ catalyst showed only two peaks which can be ascribed to nickel metal. No obvious difference in the intensity of the peaks for nickel metal was found among these catalysts. As described above, with an increase in ZrO₂ content, the intensity of peaks of ZrO₂ peaks increased. From the half peak width, the particle sizes of nickel metal and zirconia were obtained and the results are given in Table 3. It is found that the Ni/ZrO₂-Al₂O₃ catalysts have bigger particle sizes in a range of 15—20 nm for both nickel metal and zirconia.

2.2 Catalytic activity for carbon dioxide reforming of methane

The stoichiometric reforming reaction was conducted at atmospheric pressure and GHSV of 18000 ml/(g·h), and the catalytic performance of various ZrO₂-Al₂O₃ supported Ni

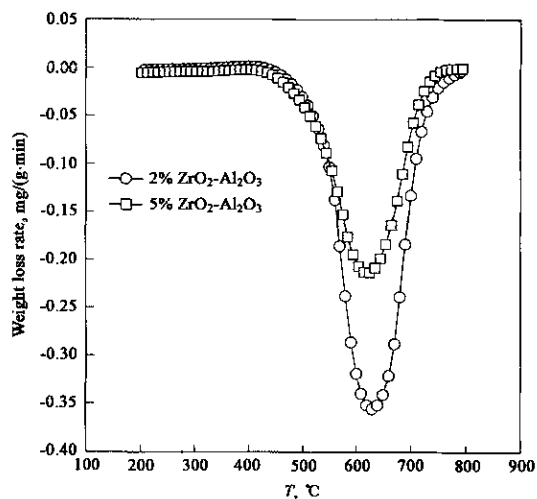
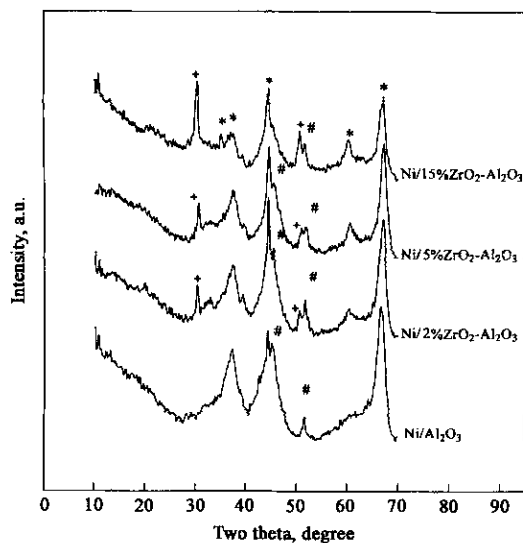


Fig. 2 Thermal stability of composite oxide supports

Fig. 3 XRD patterns of Ni/ZrO₂-Al₂O₃ catalysts
* . Al₂O₃, JCPDS86-1410; # . Ni, JCPDS87-0712; + . ZrO₂, JCPDS88-1007

catalysts was evaluated in a fixed bed reactor in the temperature range of 500–800 °C.

Table 3 Physico-chemical properties of Ni/ZrO₂-Al₂O₃ catalysts

Catalysts	Ni loading, wt%	Crystal phase	Ni particle size, nm	ZrO ₂ particle size, nm
Ni/2% ZrO ₂ -Al ₂ O ₃	9	Ni, ZrO ₂	20	17.3
Ni/5% ZrO ₂ -Al ₂ O ₃	9	Ni, ZrO ₂	14.6	16.9
Ni/15% ZrO ₂ -Al ₂ O ₃	9	Ni, ZrO ₂	14.6	13
Ni/Al ₂ O ₃	9	Ni	20.6	-
Ni/2% ZrO ₂ -Al ₂ O ₃ (used)	9	Ni, ZrO ₂ , C	-	15.1
Ni/5% ZrO ₂ -Al ₂ O ₃ (used)	9	Ni, ZrO ₂ , C	-	15

The activity results of various catalysts are shown in Table 4 and 5. It is seen obviously that the conversion increases with the rise of the reaction temperature. Comparison between CH₄ and CO₂ conversions reveals that the CO₂ conversion is generally higher than the CH₄ conversion. This is because some side reactions occur in CO₂ reforming of methane (reverse water shift reaction causes more CO₂ to be consumed). The reaction data show that the nature of support can have an impact on catalytic behaviors. The activity patterns were divided into two parts, one included Ni/2%

ZrO₂-Al₂O₃ and Ni/5% ZrO₂-Al₂O₃, another contained Ni/Al₂O₃, Ni/1% ZrO₂-Al₂O₃ and Ni/15% ZrO₂-Al₂O₃. The former is higher than the latter in the initial activity. As shown in Table 2 and 3, there were some connections among ZrO₂ content, surface area and the initial activity.

Table 4 CO₂ conversions (%) over various Ni catalysts at different temperatures

Catalyst	Reaction temperature, °C						
	500	550	600	650	700	750	800
Ni/1% ZrO ₂ -Al ₂ O ₃	16	30	48	63	77	86	90
Ni/2% ZrO ₂ -Al ₂ O ₃	22	41.2	58.4	76.2	88.7	94	95
Ni/5% ZrO ₂ -Al ₂ O ₃	20.3	39	57.1	74.1	89.3	93.2	94.1
Ni/15% ZrO ₂ -Al ₂ O ₃	17.6	34.6	50.7	70.6	81.3	90.4	93.5
Ni/Al ₂ O ₃	17.2	32	50.5	66	80	88	91

Table 5 CH₄ conversions (%) over various Ni catalysts at different temperatures

Catalyst	Reaction temperature, °C						
	500	550	600	650	700	750	800
Ni/1% ZrO ₂ -Al ₂ O ₃	12	28	42	62	76	84	90
Ni/2% ZrO ₂ -Al ₂ O ₃	17.5	33.6	51.2	70.2	85	93	93.6
Ni/5% ZrO ₂ -Al ₂ O ₃	17	37	57	71	85.2	92.3	93
Ni/15% ZrO ₂ -Al ₂ O ₃	11.5	27.1	44.4	56.4	77.4	88.6	92
Ni/Al ₂ O ₃	13.7	30	42.4	64	78	86	90

2.3 Catalytic stability

The catalytic stability experiments were conducted at 750 °C over Ni/Al₂O₃, Ni/2% ZrO₂-Al₂O₃, Ni/5% ZrO₂-Al₂O₃, and Ni/15% ZrO₂-Al₂O₃ catalysts. The variation in CO₂ and CH₄ conversions as a function of time is shown in Fig. 4. It was seen that different catalysts showed deactivation to a different extent. As clearly shown, over the testing period, Ni/2% ZrO₂-Al₂O₃ showed moderate deactivation in the reaction. The CO₂ and CH₄ conversions on Ni/2% ZrO₂-Al₂O₃ decreased from 93% and 92% to 78% and 75%. While Ni/15% ZrO₂-Al₂O₃ catalyst showed a relatively serious deactivation, its CO₂ and CH₄ conversions decreased from 90% and 88% to 74% and 72%. However, Ni/5% ZrO₂-Al₂O₃ has little deactivation during 100 h testing. The deactivation rates of these four catalysts are in following order: Ni/5% ZrO₂-Al₂O₃ < Ni/2% ZrO₂-Al₂O₃ < Ni/15% ZrO₂-Al₂O₃ < Ni/Al₂O₃. As a long reaction time of 100 h, the CO₂ and CH₄ conversions of Ni/5% ZrO₂-Al₂O₃ only decreased by about 12% and 11.5% respectively, while the drop in conversions over Ni/Al₂O₃ catalyst are 26% and 27% at 100 h. The above results indicate that ZrO₂-Al₂O₃ supported Ni catalysts have a good catalytic performance, not only a high activity, but also a relatively longer stability. Based upon the characterization results of catalyst structure and carbon deposits, and the long time reaction data. Both the carbon deposition and sintering are related to deactivation. It seems to be most likely that methane adsorbed on nickel particles and CO₂ adsorbed on support oxide zirconia. The reforming reaction of CO₂ with CH₄ is expected to proceed at the interface of nickel and zirconia by the following steps: (1) dehydrogenation of methane to form surface carbon and hydrogen; (2) dissociative adsorption of CO₂, and (3) reduction of CO₂ to CO. The catalyst composites small size zirconia and well dispersed nickel particles with small size, perhaps has this nano composite structure of active phase (Ni) and support (zirconia) is beneficial to prevent to carbon deposit and sintering.

2.4 Deactivation of catalysts and carbon deposition

From Table 2, it can be seen that for Ni/2% ZrO₂-Al₂O₃ and Ni/5% ZrO₂-Al₂O₃ catalysts, the surface area and pore volume decreased after use, but the average pore size

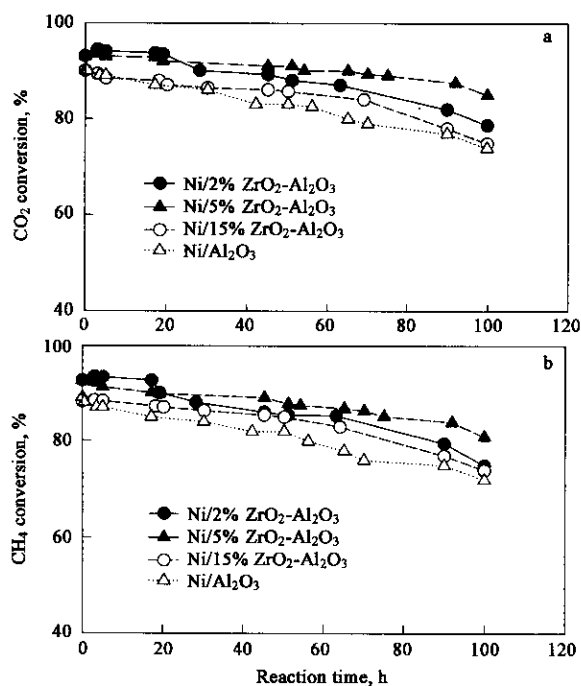


Fig. 4 Deactivation testing of the catalysts in a fixed-bed at 750°C. Reaction conditions: $CH_4/CO_2 = 1/1$, $P = 1$ atm, flow rate = 60 ml/min

increased after a long-period reaction. This change to large pore range indicates that the pores were gradually blocked by the carbon deposition.

Fig. 5 shows the XRD patterns of fresh and used Ni/2% $ZrO_2-Al_2O_3$ and Ni/5% $ZrO_2-Al_2O_3$ catalysts. As described above, except for the diffraction peaks of Al_2O_3 , the fresh catalysts showed peaks of nickel metal and zirconia. After a relatively long time of reaction, no appreciable difference in the intensity of peaks of nickel metal and zirconia is found. A new peak appears which can be ascribed to carbon, clearly indicating that there was carbon deposition on the catalyst surface. As discussed above, the composite oxide supports possess a relatively higher stability at high temperatures. Therefore sintering deactivation is negligible deactivation compared to deactivation due to carbon deposition.

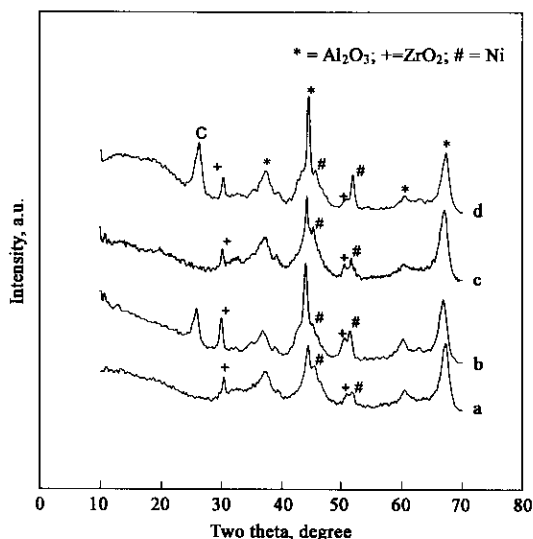


Fig. 5 XRD patterns of Ni/ $ZrO_2-Al_2O_3$ catalysts before and after reaction a. Ni/5% $ZrO_2-Al_2O_3$ (fresh); b. Ni/5% $ZrO_2-Al_2O_3$ (used for 100 h); c. Ni/2% $ZrO_2-Al_2O_3$ (fresh); d. Ni/2% $ZrO_2-Al_2O_3$ (used for 100 h)

The surface carbon concentration of used catalysts was analyzed by the XPS technique. The C_{1s} spectra are shown in Fig. 6. It is apparent that there were carbon deposits on these

catalysts after reaction. The concentration of surface carbon is much lower on Ni/5% $ZrO_2-Al_2O_3$ than that on Ni/1% $ZrO_2-Al_2O_3$ and Ni/2% $ZrO_2-Al_2O_3$ catalysts. The former shows lower surface carbon deposition. For these catalysts, C_{1s} envelope is predominately at a signal peak at 285 eV, with a minor shoulder sloping to higher BE at 292 eV, which can be ascribed to C-C and CO_3^- components, respectively.

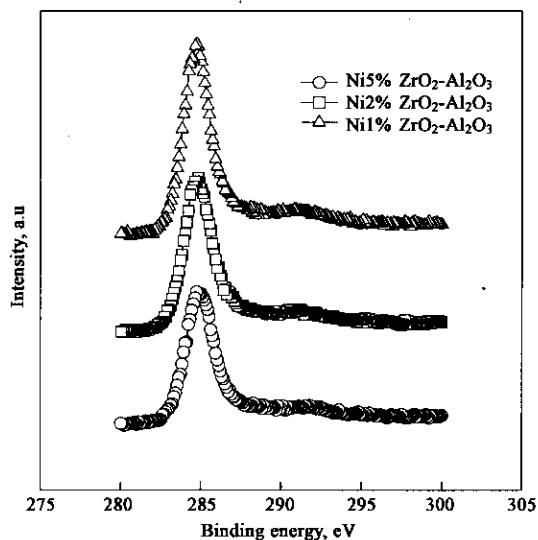


Fig. 6 C_{1s} spectra of various Ni catalysts after reaction

The amount of carbon deposited on the catalysts in deactivation tests was measured by temperature program oxidation (TPO) experiments in TGA. The weight loss profile between 400°C and 800°C is presented in Fig. 7. It is seen that carbon began to be oxidized at 450°C, but their peaks appeared at different temperatures. Carbon on Ni/1% $ZrO_2-Al_2O_3$ showed the maximum oxidation rate around 640°C, the peak of Ni/2% $ZrO_2-Al_2O_3$ centered at 637°C, and the oxidation of carbon on the Ni/5% $ZrO_2-Al_2O_3$ showed a peak at about 612°C. The amount of carbon calculated indicated that the Ni/5% $ZrO_2-Al_2O_3$ had the lowest coking activity, while Ni/1% $ZrO_2-Al_2O_3$ showed the highest coking among these catalysts.

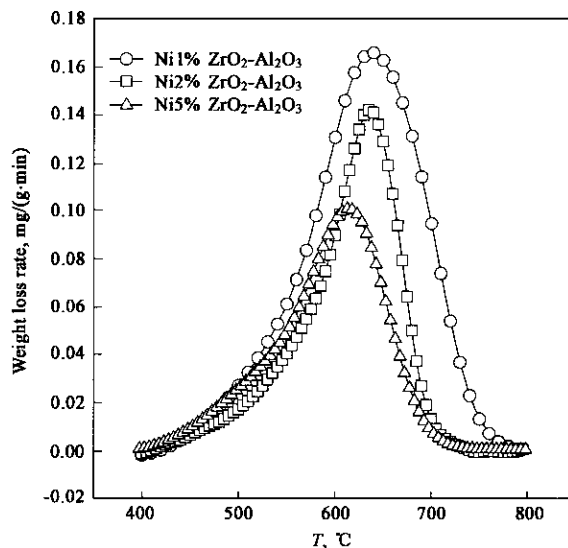


Fig. 7 TPO profiles of carbonaceous species formed on the catalysts after reaction at 750°C

Oxides, either as promoters or in composite supports, were added to the supported nickel catalysts in order to

improve the catalytic performances for the carbon dioxide reforming of methane. It has been reported that addition of alkali, alkaline earth and rare earth oxides to Ni/Al₂O₃ catalysts could change the catalytic behaviors. Zhang (Zhang, 1994) has found that the addition CaO of to Ni/Al₂O₃ catalyst resulted in an increase in activity. The rate of enhancement appeared to be related to the enhanced reducibility of Ni dispersed on CaO/Al₂O₃ support. It was reported by Cheng *et al.* (Cheng, 1996) that La₂O₃ and CeO₂ promoted Ni/Al₂O₃ catalysts had enhanced activities. It was observed by Wang and Lu (Wang, 1997) that Na₂O and MgO oxides decreased the activity of Ni/Al₂O₃ catalyst, and these catalysts also showed some degree of deactivation. In contrast, CaO, La₂O₃ and CeO₂ enhanced both activity and stability of Ni/Al₂O₃ catalyst. In this investigation, addition of zirconia, did not reduce greatly the surface area and pore volume of Al₂O₃ support. As shown in Table 3, in particular, the oxide increased the nickel dispersion on catalysts, which explain the higher activity than with the Ni/Al₂O₃ catalyst. Perhaps the lesser occurrence of sintering of nickel and zirconia and higher coking resistance is responsible for the higher stability. The suppression of carbon deposition could partly be ascribed to the basicity of zirconia added.

3 Conclusions

This work showed that ZrO₂-Al₂O₃ composite oxide is a promising catalyst support for the methane reforming of carbon dioxide. The composite support phase and pore structure influenced the catalytic performance. An increase in the catalytic activity and stability of methane and carbon dioxide reforming reaction is resulted from the addition of zirconia. Ni/5% ZrO₂-Al₂O₃ was better than Ni/2% ZrO₂-Al₂O₃ and Ni/15% ZrO₂-Al₂O₃ catalysts, in terms of catalytic conversion and stability. The catalyst has a strong resistance to sintering, and the carbon deposition is responsible for the final deactivation after a relatively long-period reaction.

Acknowledgements: The authors thank Dr. B. Wood of the Department of Chemistry for the XPS measurements, and Mr. L. K. Bekessy of the Department of Mining and Material Engineering for XRD measurements.

References:

- Bradford M C J, Vannice M A, 1999. CO₂ reforming of CH₄[J]. *Catal Rev*, 41: 1—42.
- Cheng Z X, Wu Q, Li J L *et al.*, 1996. Effects of promoters and preparation procedures on reforming of methane with carbon dioxide over Ni/Al₂O₃ catalysts[J]. *Catal Today*, 10: 147—155.
- Chudhary V R, Uphade B S, Mamman A S, 1995. Large enhancement in methane to syngas conversion activity of supported Ni catalysts due to pre-coating of supported with MgO, CaO or rare earth oxide[J]. *Catal Lett*, 32: 387—390.
- Guo Y, Li S B, Zhang B *et al.*, 2000. Influence of ZrO₂ on carbon monoxide oxidation over Pd/Al₂O₃[J]. *React Kinet Catal Lett*, 69: 153—159.
- Hao Z P, Zhu H Y, Lu G Q, 2003. Zr-laponite pillared clay-based nickel catalysts for methane reforming with carbon dioxide[J]. *Appl Catal A*, 242: 275—286.
- Lercher J A, Bitter J H, Hally W *et al.*, 1996. Design of stable catalyst for methane-carbon dioxide reforming[J]. *Stud Surf Sci Catal*, 101: 463—473.
- Li X S, Chang J S, Park S E, 1999a. CO₂ reforming of methane over zirconia-supported nickel catalysts: (1) Catalytic specificity[J]. *React Kinet Catal Lett*, 67: 375—382.
- Li X S, Chang J S, Lee E K *et al.*, 1999b. CO₂ reforming of methane over zirconia-supported nickel catalysts: (2) Thermogravimetric analysis [J]. *React Kinet Catal Lett*, 67: 383—390.
- Ruckenstein E, Hu Y H, 1996. Interaction between Ni and La₂O₃ in Ni/La₂O₃ catalysts prepared using different Ni precursors[J]. *J Catal*, 161: 55—61.
- Seshan K, Barge H M, Hally W *et al.*, 1994. Carbon dioxide reforming of methane in the presence of nickel and platinum catalysts supported on ZrO₂ [J]. *Stud Surf Sci Catal*, 81: 285—290.
- Wang S B, Lu G Q, 1997. Effects of oxide promoters on metal dispersed and metal-support interaction in Ni catalysts supported on carbon[J]. *Ind Eng Chem Res*, 30: 5103—5109.
- Wang S B, Lu G Q, 1998. CO₂ reforming of methane on Ni catalysts: Effect of the support phase and preparation technique[J]. *Appl Catal B*, 16: 269—277.
- Wang S B, Lu G Q, 1999. A comprehensive study on carbon dioxide reforming of methane over Ni/γ-Al₂O₃ catalysts[J]. *Ind Eng Chem Res*, 38: 2615—2625.
- Wei J M, Xu B Q, Li J L *et al.*, 2000. High active and stable Ni/ZrO₂ catalyst for syngas production by carbon dioxide reforming of methane [J]. *Appl Catal A*, 167: 39—48.
- Zhang R, Schwarz J A, Datye A *et al.*, 1992. The effect of second-phase oxide on the catalytic properties of dispersed metal[J]. *J Catal*, 138: 55—69.
- Zhang Z L, Verykios X E, 1994. Carbon dioxide reforming of methane to synthesis gas over supported Ni catalysts[J]. *Catal Today*, 21: 589—595.
- Zhang Z L, Tsiopourari V A, Efsthathiou A M *et al.*, 1996. Reforming of methane with carbon dioxide to synthesis gas over supported rhodium catalysts[J]. *J Catal*, 158: 51—61.

(Received for review January 21, 2003. Accepted June 5, 2003)